2914 *Organometallics* **2006,** *25,* 2914−2916

Novel Heterobimetallic Metallamacrocycles Based on the 1,1′-Bis(1,8-naphthyrid-2-yl)ferrocene ($\mathrm{FcNP_2}$) Ligand: Structural Characterization of the Complexes $[\{\mathrm{M(FcNP_2)}\}_2]^{2+}$ (M = $\mathrm{Cu^I}$, $\mathrm{Ag^I}$) and $\{\mathrm{MCl_2(FcNP_2)}\}_4$ (M = $\mathrm{Zn^{II}}$, $\mathrm{Co^{II}}$)

Nabanita Sadhukhan, Sanjib K. Patra, Kasinath Sana, and Jitendra K. Bera*

Department of Chemistry, Indian Institute of Technology, Kanpur, India 208016

Received March 21, 2006

Summary: Self-assembly reactions of 1,1′-bis(1,8-naphthyrid-2-yl)ferrocene ($FcNP_2$) with Cu^I/Ag^I afford dimeric $[\{Cu^I/Ag^I(FcNP_2)\}_2]^{2+}$ and with $ZnCl_2$/$CoCl_2$ yield tetrameric metallamacrocycles $\{Zn^{II}/Co^{II}Cl_2(FcNP_2)\}_4$.

The field of inorganic supramolecular chemistry is motivated to a large extent by a desire to create new types of molecular architecture.[1] This prospect, however, lies in our ability to prepare functionally important materials. Ferrocene-based ligands are attractive candidates for building novel structural motifs owing to the conformational flexibility of the ferrocenyl rings.[2] The evaluation of electrochemical, optical, and catalytic properties of ferrocene-containing materials is a major topic of current research.[3] Organometallic ligands having two N-heterocyclic units joined by a ferrocene spacer have been employed in conjunction with transition metal ions to generate discrete molecular assemblies. The disposition of N atoms and the identity of metal ions dictate the topology of the products. Octamethyl-5,5′-bis(2-pyridyl)ferrocene ($\mathrm{Fc^*(py\text{-}2)_2}$), for example, binds $\mathrm{Cu^I}$ to form a chelate complex,[4] whereas 1,1′-bis(4-pyridyl)ferrocene ($\mathrm{Fc(py\text{-}4)_2}$) forms a metallamacrocycle involving two bidentate ligands connected by two $\mathrm{Ag^I}$/$\mathrm{Cu^{II}}$ ions.[5] The demonstrated ability of the 1,8-naphthyridine (NP) units to bind metal ions in different modes, including monodentate, bidentate chelating, or binuclear bridging, prompted the utilization of Fc-NP hybrids in building metalla-supramolecular architectures.[6]

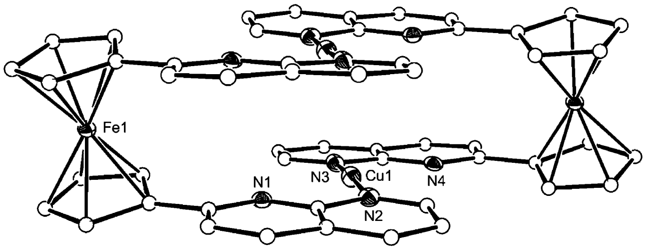

Figure 1. Molecular structure of the dicationic unit $[\{\mathrm{Cu(FcNP_2)}\}_2]^{2+}$ in **1** with important atoms labeled. Carbon atoms are shown as circles of arbitrary radius. Selected bond distances (Å) and angles (deg): Cu1···Cu1 3.268(1), Fe···Fe 11.104(3), Cu1−N2 1.889(3), Cu1−N3 1.898(3), N2−Cu1−N3 176.47(13).

Friedlander condensation of 1,1′-diacetylferrocene with 2 equiv of 2-aminonicotinaldehyde in methanolic potassium hydroxide provides 1,1′-bis(1,8-naphthyrid-2-yl)ferrocene (abbreviated as $\mathrm{FcNP_2}$).[7] The reactions of $\mathrm{FcNP_2}$ with $\mathrm{CuClO_4}$ and AgOTf afforded dimeric $[\{\mathrm{Cu(FcNP_2)}\}_2][\mathrm{ClO_4}]_2$ (**1**) and $[\{\mathrm{Ag(FcNP_2)}\}_2][\mathrm{OTf}]_2$ (**2**), and with $\mathrm{CoCl_2}$ and $\mathrm{ZnCl_2}$ resulted in the tetrameric isostructural $\{\mathrm{MCl_2(FcNP_2)}\}_4$ (**3**, M = Zn; **4**, M = Co), respectively.[8]

Compound **1** is formed in the reaction of $\mathrm{FcNP_2}$ and $\mathrm{CuClO_4}$ regardless of ligand-to-metal ratio. The molecular structure of the dicationic unit $[\{\mathrm{Cu(FcNP_2)}\}_2]^{2+}$ consists of two $\mathrm{FcNP_2}$ molecules bridged by two Cu atoms as shown in Figure 1.[9] Each Cu atom is coordinated to two distal N atoms from two $\mathrm{FcNP_2}$ units in a quasi-linear environment with Cu−N distances of 1.889(3) and 1.898(3) Å and N2−Cu1−N3 angle of 176.47(13)°. The Cu···Cu separation of 3.268(1) Å in **1** is shorter than the corresponding distances of 3.428(5) and 3.473(5) Å noted in two independent molecules of $[\{\mathrm{Fc(py\text{-}4)_2Cu(OAc)_2}\}_2]^{2+}$.[5] The coordinated acetates in the latter complex suppress any likely

---

* To whom correspondence should be addressed. E-mail: jbera@iitk.ac.in.

[1] (a) Bera, J. K.; Bacsa, J.; Dunbar, K. R. *Encyclopedia of Inorganic Chemistry*, 2nd ed.; King, R. B., Ed.; John Wiley & Sons: New York, 2005. (b) Holliday, B. J.; Mirkin, C. A. *Angew. Chem., Int. Ed.* **2001**, *40*, 2022. (c) Olenyuk, S. B.; Stang, P. J. *Chem. Rev.* **2000**, *100*, 853. Fujita, M. *Chem. Soc. Rev.* **1998**, *27*, 417.

[2] (a) Li, M.; Bai, Y.; Zhang, B.; Duan, C.; Xu, J.; Meng, Q. *Inorg. Chem.* **2005**, *44*, 5459. (b) Braga, D.; Polito, M.; Bracaccini, M.; D'Addario, D.; Tagliavini, E.; Sturba, L.; Grepioni, F. *Organometallics* **2003**, *22*, 2142. (c) Reger, D. L.; K. Brown, J.; Gardinier, J. R.; Smith, M. D. *Organometallics* **2003**, *22*, 4973. (d) Chandrasekhar, V.; Nagendran, S.; Bansal, S.; Kozee, M. A.; Powell, D. R. *Angew. Chem., Int. Ed.* **2000**, *39*, 1833.

[3] Togni, A.; Hayashi, T. *Ferrocenes: Homogeneous Catalysis, Organic Synthesis, Material Science*; VCH: Weinheim, Germany, 1995.

[4] Neumann, B.; Siemeling, U.; Stammler, H.-G.; Vorfeld, U.; Delis, J. G. P.; van Leeuwen, P. W. N. M.; Vrieze, K.; Fraanje, J.; Goubitz, K.; de Biani, F. F.; Zanello, P. *J. Chem. Soc., Dalton Trans.* **1997**, 4705.

[5] (a) Braga, D.; Polito, M.; D'Addario, D.; Tagliavini, E.; Proserpio, D. M.; Grepioni F.; Steed, J. W. *Organometallics* **2003**, *22*, 4532. (b) Braga, D.; Polito, M.; Bracaccini, M.; D'Addario, D.; Tagliavini, E.; Proserpio, D. M.; Grepioni, F. *Chem. Commun.* **2002**, 1080.

[6] (a) Nakajima, H.; Nagao, H.; Tanaka, K. *J. Chem. Soc., Dalton Trans.* **1996**, 1405. (b) Munakata, M.; Maekawa, M.; Kitagawa, S.; Adachi, M.; Masuda, H. *Inorg. Chim. Acta* **1990**, *167*, 181. (c) Tsuda, T.; Ohba, S.; Takahashi, M.; Ito, M. *Acta Crystallogr., Sect. C: Cryst. Struct. Commun.* **1989**, *45*, 887. (d) Tikkanen, W. R.; Krüger, C.; Bomben, K. D.; Jolly, W. L.; Kaska, W. C.; Ford, P. C. *Inorg. Chem.* **1984**, *23*, 3633. (e) Staniewicz, R. J.; Hendricker, D. G. *J. Am. Chem. Soc.* **1977**, *99*, 6581.

[7] (a) Pastene, R.; Bozec, H. L.; Moya, S. A. *Inorg. Chem. Commun.* **2000**, *3*, 376. (b) Gelin, F.; Thummel, R. P. *J. Org. Chem.* **1992**, *57*, 3780.

[8] Synthesis of $[\{\mathrm{Cu(FcNP_2)}\}_2][\mathrm{ClO_4}]_2$ (**1**): A mixture of $\mathrm{FcNP_2}$ (20 mg, 0.046 mmol) and $[\mathrm{Cu(CH_3CN)_4}][\mathrm{ClO_4}]$ (13 mg, 0.040 mmol) was stirred in $\mathrm{CH_3CN}$ for 8 h. The solution was subsequently concentrated, and $\mathrm{CH_2Cl_2}$ was added to induce precipitation. A red solid was collected by filtration, washed with $\mathrm{CH_2Cl_2}$, and dried in a vacuum. Yield: 38 mg (81%). Single crystals were grown by diffusion of $\mathrm{Et_2O}$ onto a $\mathrm{CH_3NO_2}$ solution of **1**. $[\{\mathrm{Ag(FcNP_2)}\}_2][\mathrm{OTf}]_2$ (**2**): The reaction of $\mathrm{FcNP_2}$ (20 mg, 0.046 mmol) and AgOTf (10 mg, 0.041 mmol) was carried out following a procedure similar to that described for the synthesis of compound **1**. Yield: 40 mg (75%). Single crystals were grown by diffusion of $\mathrm{Et_2O}$ onto a $\mathrm{CH_3NO_2}$ solution of **2**. $\{\mathrm{ZnCl_2(FcNP_2)}\}_4$ (**3**) and $\{\mathrm{CoCl_2(FcNP_2)}\}_4$ (**4**): An acetonitrile solution (5 mL) of $\mathrm{ZnCl_2}$ (15 mg, 0.11 mmol) was carefully layered onto a $\mathrm{CH_3OH}$ solution (5 mL) of $\mathrm{FcNP_2}$ (6 mg, 0.014 mmol). After 7 days the resultant red crystals of **3** were isolated by filtration. Yield: 40 mg (63%). A similar procedure was carried out using $\mathrm{CoCl_2}$ (15 mg, 0.12 mmol) and 10 mg of $\mathrm{FcNP_2}$ (0.023 mmol) for the synthesis of compound **4**. Yield: 34 mg (51%).

10.1021/om060252u CCC: \$33.50

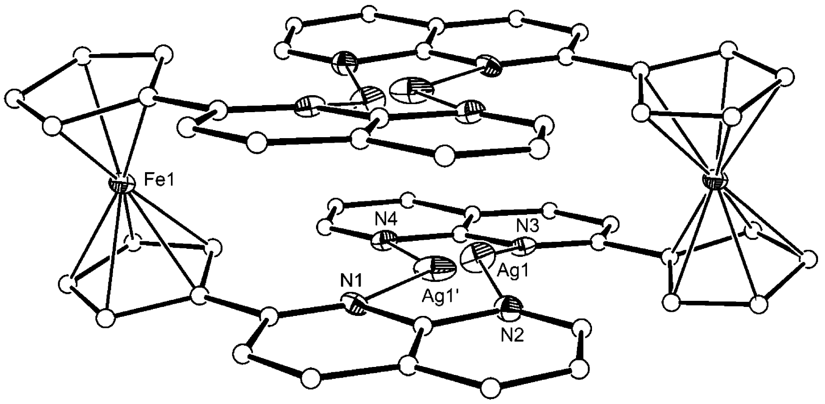

Figure 2. Molecular structure of the dicationic unit $[\{Ag(FcNP_2)\}_2]^{2+}$ in **2** with important atoms labeled. Carbon atoms are shown as circles of arbitrary radius. Selected bond distances (Å) and angles (deg): Fe1$\cdots$Fe1 9.127(1), Ag1$\cdots$Ag1 3.187(2), Ag1−N3 2.205(4), Ag1−N2 2.311(4), Ag1′−N1 2.319(4), Ag1′−N4 2.471(4) and Ag1′−N3 2.425(4), N2−Ag1−N3 146.21(14), N1−Ag1′−N4 129.27(14).

$Cu^{II}\cdots Cu^{II}$ interaction, leading to a longer metal−metal distance. The rectangular-shaped metallamacrocycles made of ferrocene sides (Fe$\cdots$Fe 11.104(3) Å) spanned by NP−Cu−NP units form one-dimensional sheets in a crystal that are aggregated to form a two-dimensional structure by $\pi-\pi$ stacking interactions involving intermolecular Cp$\cdots$Cp and Cp$\cdots$NP rings (cf. Figure S1 in the Supporting Information).

The structure of the $[\{Ag(FcNP_2)\}_2]^{2+}$ unit in complex **2** obtained from the reaction of $FcNP_2$ with AgOTf is shown in Figure 2. Although the basic structural features are similar to that of Cu^I complex **1**, significant differences in the coordination of the metal ions are observed. The Ag atom was found to be disordered over two positions, separated by 0.696(1) Å, with occupancies of 0.62 (Ag1) and 0.38 (Ag1′), surrounded by two NP units from two $FcNP_2$. The Ag1−N and Ag1′−N distances that are shorter than 2.50 Å are listed in the figure caption. The highlight of the $[\{Ag(FcNP_2)\}_2]^{2+}$ structure is the head-on arrangements of the NP units, stemming from Ag^I coordination, leading to a metallacycle that is significantly smaller in width (Fe$\cdots$Fe 9.127(1) Å) in comparison to "$[\{Cu(FcNP_2)\}_2]$" in **1**.

Reactions of $ZnCl_2$ and $CoCl_2$ with $FcNP_2$ provide isostructural **3** and **4**. The molecular structure of the discrete $\{ZnCl_2(FcNP_2)\}_4$, composed of alternating $ZnCl_2$ and $FcNP_2$ units, is shown in Figure 3. Each "$ZnCl_2$" is bonded to two distal N atoms of different $FcNP_2$. The overall structure of the metallamacrocycle **3** is described to consist of a Zn_4 square of dimensions 9.584(2) Å spanned by $FcNP_2$ units. The Fc units are alternatively above and below the plane of the Zn_4 square, forming an Fe_4 tetrahedron consisting of four isosceles triangles with Fe$\cdots$Fe distances of 9.271(3) and 7.844(2) Å. Each Fe atom is connected to two neighboring Zn by Cp−NP units with Fe$\cdots$Zn distances of 5.995(2) and 6.261(2) Å (cf. Figure S3 in the Supporting Information).

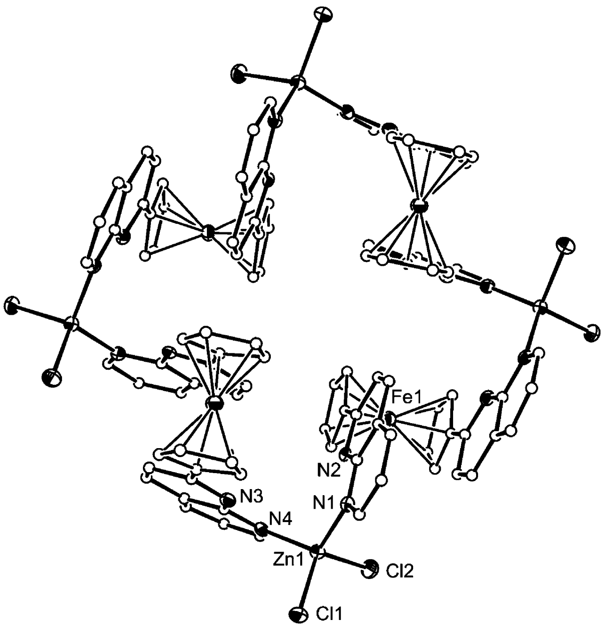

Figure 3. Molecular structure of $\{ZnCl_2(FcNP_2)\}_4$ (**3**) with important atoms labeled. Carbon atoms are shown as circles of arbitrary radius. Selected bond distances (Å) and angles (deg): Zn1$\cdots$Zn1 9.584(2), Fe1$\cdots$Fe1(A) 9.271(3), Fe1$\cdots$Fe1(B) 7.844(2), Zn1$\cdots$Fe1 5.995(2), Zn1$\cdots$Fe1(A) 6.261(2), Zn1−N1 2.050(4), Zn1−N4 2.045(4), Zn1−Cl1 2.259(2), Zn1−Cl2 2.254(2), N1−Zn1−N4 117.1(2), Cl1−Zn1−N1 103.3(1), Cl2−Zn1−N1 108.3(1), Cl1−Zn1−N4 111.3(1), Cl2−Zn1−N4 103.8(1), Cl1−Zn1−Cl2 113.37(5). Symmetry codes A: $0.5-x, y-0.5, 1.5-z$; B: $-x, 1-y, z$.

The conformations of the Cp−NP units, as guided by the metal ions, shape the structures of the macrocycles. The Cp−NP units in **1** and **2** adopt a near-eclipsed conformation (Figure 4a) different from the antiperiplanar orientation of the Cp rings in free $FcNP_2$.[10] The conformation of the Cp rings in **3** is synperiplanar. The tetrahedral geometry of the Zn^{II}, however, forces the NP rings to adopt a staggered conformation, as shown in Figure 4b. The Zn1−N1−N4(C)−Zn1(C) (symmetry code C: $0.5 + x, 0.5 - y, 1.5 - z$) torsion angle of 56.3(3)° in **3** and the corresponding Cu1−N2−N3(D)−Cu1(D) (symmetry code D: $-x, 1 - y, 1 - z$) torsion angle of 0.5(1)° in **1** illustrate the directionalities of N lone pairs in the respective compounds.

Incorporation of two NP units onto ferrocene causes a significant shift of ferrocene-based oxidation toward more positive potential in the cyclic voltammogram (CV) of $FcNP_2$, exhibiting a reversible 1e^- oxidation wave at 0.66(100) V. The

---

(9) Crystal data for **1**·4(CH_3NO_2): formula $C_{56}H_{48}Cl_2Cu_2Fe_2N_{12}O_{16}$, triclinic, space group $P\bar{1}$, $a = 7.5414(15)$ Å, $b = 13.316(3)$ Å, $c = 14.109(3)$ Å, $\alpha = 93.81(3)°$, $\beta = 95.46(3)°$, $\gamma = 93.56(3)°$, $V = 1403.9(5)$ Å^3, 9425 reflections collected, 6678 unique, GooF = 0.970, R1 = 0.0526, wR2 = 0.1128. Crystal data for **2**·2(CH_3NO_2): formula $C_{56}H_{42}Ag_2F_6Fe_2N_{10}O_{10}S_2$, monoclinic, space group $P2_1/n$, $a = 16.9157(13)$ Å, $b = 7.3260(6)$ Å, $c = 21.3936(18)$ Å, $\beta = 95.010(2)°$, $V = 2641.1(4)$ Å^3, 17 031 reflections collected, 6467 unique, GooF = 1.015, R1 = 0.0594, wR2 = 0.1210. Crystal data for **3**·4(CH_3CN): formula $C_{112}H_{84}Cl_8Fe_4N_{20}Zn_4$, tetragonal, space group $I\bar{4}$, $a = b = 21.268(5)$ Å, $c = 11.459(5)$ Å, $V = 5183(3)$ Å^3, 17 275 reflections collected, 6373 unique, GooF = 1.091, R1 = 0.0542, wR2 = 0.1037. Details of the data collection and refinement parameters are given in the Supporting Information.

(10) (a) Dong, G.; Yu-ting, L.; Chun-ying, D.; Hong, M.; Qing-jin, M. *Inorg. Chem.* **2003**, *42*, 2519. (b) Rheingold, A. L.; Mueller-Westerhoff, U. T.; Swiegers, G. F.; Haas, T. J. *Organometallics* **1992**, *11*, 3411.

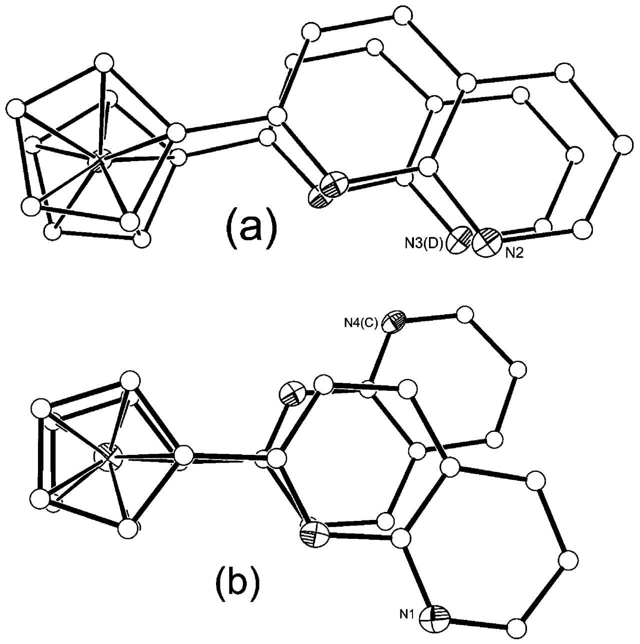

Figure 4. Conformation of Cp−NP units in **1** (a) and in **3** (b).

CV of **1** in propylene carbonate shows an oxidation wave at 0.80 V corresponding to a double 1e$^-$ transfer from the two equivalent ferrocene units. The separation of the anodic oxidation peak and the cathodic counter peak is 150 mV when measured at a scan rate of 100 mV/S. An additional Cu^{I}/Cu^{II} oxidation appears at $E_{p,a}$ +0.33 V. The NP-based irreversible reduction potential $E_{p,c}$ is observed at −1.83 V. The CV indicates that the ferrocene and NP units are noninteracting equivalent redox centers despite linking by Cu^{I}.[11] Compound **2** shows similar electrochemical behavior with ferrocene based oxidation at 0.70(100) V and a NP-based reduction wave at −1.88 V. The CVs of both the compounds are marred by unusually small peak separation of the oxidation wave and by the appearance of a sharp anodic current wave when multiple voltage scans are executed, indicating adsorption phenomena on the electrode surface. The low solubility of compounds **3** and **4** did not allow us to carry out electrochemical studies.

Compounds **1** and **2** exhibit identical emission spectra with two peaks at 415 and 437 nm of equal intensities in the solid state measured at room temperature upon excitation at around 368 nm. Compound **3** has a broad emission ranging from 385 to 550 nm, with the maximum intensity at 424 nm, and the corresponding excitation maximum is at 353 nm (Figure 5). The emission spectrum of **4** exhibits double peaks at $\lambda_{max} = 417$ and 438 nm. We assign the emissions primarily to intraligand $^1\pi-\pi^*$ fluorescence since similar emission peaks with λ_{max} values at 419 and 440 nm are observed for pristine FcNP$_2$. The absence of the double peaks for **3** tends to suggest an emissive state with significant Zn^{II} character.

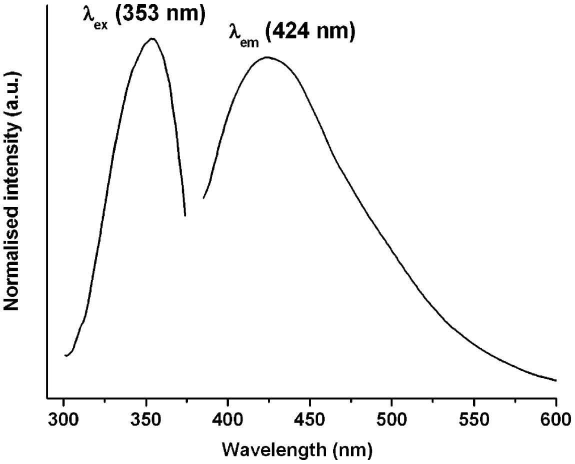

Figure 5. Excitation and emission spectra of **3** in the solid state at RT.

This study illustrates the feasibility of constructing metallamacrocycles of interesting topology based on the self-assembly of FcNP$_2$ with linear two-coordinate and tetrahedral metal ions. The advantage of FcNP$_2$ over its pyridyl congener in making complex architectures has been demonstrated. Efforts are underway to incorporate square-planar and octahedral metal ions in the design of new types of structures. The prospect of FcNP$_2$ to engage a multiply bonded dimetal unit in a bidentate bridging mode is being actively pursued in our laboratory.

Acknowledgment. J.K.B. thanks the DST India for support of this research. N.S. thanks the CSIR India for a fellowship. The authors thank Dr. S. P. Rath for valuable advice on X-ray crystallography.

Supporting Information Available: Details of the crystal data and refinement parameters, conformations of the Cp−NP units in the compounds, crystal-packing diagrams, thermal ellipsoid diagrams, cif files of the structures, tables of electrochemical data, and emission spectra of compounds FcNP$_2$, **1**−**4**. This material is available free of charge via the Internet at http://pubs.acs.org.

OM060252U

---

[11] (a) Paolucci, D.; Marcaccio, M.; Bruno, C.; Braga, D.; Polito, M.; Paolucci, F.; Grepioni, F. *Organometallics* **2005**, *24*, 1198. (b) Das, N.; Arif, A. M.; Stang, P. J.; Sieger, M.; Sarkar, B.; Kaim, W.; Fiedler, J. *Inorg. Chem.* **2005**, *44*, 5798.